

Probing the trilinear Higgs boson self-coupling via single Higgs production at the LHeC

Ruibo Li ^{a,*} Xiao-Min Shen ^{a,†} Bo-Wen Wang ^{a,‡} Kai Wang ^{a,§} and Guohuai Zhu ^{a,¶}

^a *Zhejiang Institute of Modern Physics, Department of Physics,
Zhejiang University, Hangzhou, Zhejiang 310027, CHINA*

Abstract

The determination of the Higgs self coupling is one of the key ingredients for understanding the mechanism behind the electroweak symmetry breaking. An indirect method for constraining the Higgs trilinear self coupling via single Higgs production at next-to-leading order (NLO) has been proposed in order to avoid the drawbacks of studies with double Higgs production. In this paper we study the Higgs self interaction through the vector boson fusion (VBF) process $e^-p \rightarrow \nu_e h j$ at the future LHeC. At NLO level, we compute analytically the scattering amplitudes for relevant processes, in particular those induced by the Higgs self interaction. A Monte Carlo simulation and a statistical analysis utilizing the analytic results are then carried out for Higgs production through VBF and decay to $b\bar{b}$, which yield for the trilinear Higgs self-coupling rescaling parameter κ_λ the limit $[-0.28, 4.25]$ with 2 ab^{-1} integrated luminosity. If we assume 10% of the signal survives the event selection cuts, and include all the background, the constraint will be broadened to $[-1.95, 5.93]$.

*Electronic address: bobli@zju.edu.cn

†Electronic address: xmshen@zju.edu.cn

‡Electronic address: 0617626@zju.edu.cn

§Electronic address: wangkai1@zju.edu.cn

¶Electronic address: zhugh@zju.edu.cn

I. INTRODUCTION

A standard model (SM)-like Higgs boson has been discovered by the ATLAS and CMS collaborations at the CERN Large Hadron Collider (LHC) individually [1, 2], which makes a milestone in particle physics. While it strongly supports the SM mechanism of spontaneous electroweak symmetry breaking (EWSB), by which all fermions and some of the vector bosons acquire their masses, the driven force of EWSB still remains mysterious. To better understand this problem, it is crucial to study the properties of the Higgs boson, e.g., to measure its mass, spin, CP properties and couplings [3–6]. From the second run of the LHC at 13 TeV, the ATLAS collaboration has recently reported the results of their measurements $\mu_{H \rightarrow \tau\tau} = 1.09_{-0.30}^{+0.36}$ and $\mu_{H \rightarrow bb} = 1.01_{-0.19}^{+0.20}$, with the integrated luminosities 36.1 fb^{-1} and 79.8 fb^{-1} , respectively [7, 8]. These are significant improvements in Higgs precision physics.

However, the study of the Higgs self-coupling (λ) from the scalar potential $V(\Phi)$ is in a completely different situation. After EWSB the scalar potential takes a form with the trilinear ($\lambda_3^{SM} = \lambda$) and quartic ($\lambda_4^{SM} = \lambda/4$) self interactions:

$$V(\Phi) = -\mu^2 \Phi^\dagger \Phi + \lambda (\Phi^\dagger \Phi)^2 \rightarrow \frac{1}{2} m_h^2 h^2 + \lambda_3 \nu h^3 + \lambda_4 h^4 \quad (1)$$

where Φ is the Higgs doublet field and h is the Higgs boson. At the LHC, double Higgs production as the standard process for determining the Higgs trilinear self coupling suffers from a small production rate and huge QCD backgrounds, and thus leads to large uncertainties even after the Run-II upgrade. The measurements of the $\gamma\gamma b\bar{b}$ final states by the CMS and ATLAS experiments yield the constraints $-11\lambda_3^{SM} < \lambda_3 < 17\lambda_3^{SM}$ and $-8.2\lambda_3^{SM} < \lambda_3 < 13.2\lambda_3^{SM}$, respectively [9, 10]. For the $b\bar{b}b\bar{b}$ production, the observed upper limit by ATLAS using the non-resonant Higgs pair production data is 13 times the SM value at 95% C.L [11]. There are also extensive phenomenological studies on determining the trilinear Higgs self-coupling directly at the LHC [12–21], the future electron-positron collider [22–25], and future high energy hadron colliders [26–34], in which strict constraints are obtained with higher integrated luminosities and energies. On the other hand, an indirect method is proposed for constraining the Higgs self-coupling via single Higgs production at next-to-leading order (NLO) [24, 35–39]. The method relies on the account of one-loop electroweak radiative corrections to Higgs-strahlung and vector boson fusion (VBF) processes [40–43], and it has the potential of reaching a superior precision in the determination of the Higgs self-coupling, as compared to the determination via double Higgs production.

In view of the large QCD backgrounds interfering with the one-loop electroweak radiative corrections at the hadron-hadron collider, the Large Hadron electron Collider (LHeC) has been proposed as a deep inelastic scattering facility for the precision measurement of parton distributions and Higgs properties. LHeC as a relatively economic proposal is an upgrade based on the current 7 TeV proton beam of the LHC by adding one electron beam with 60–140 GeV energy [44], which could be tuned into a “Higgs factory” in which Higgs bosons are produced via VBF process. Thanks to the forward detector and reduction of QCD backgrounds in the e - p collider, the bottom Yukawa and trilinear Higgs self couplings could be measured precisely [45–47]. Therefore, we expect the LHeC to be a good facility for studying λ_3 via single Higgs production at NLO level.

The paper is organised as follows. In the next section, we discuss the one-loop contribution to single Higgs production, in particular that from processes via the trilinear Higgs self interaction and Higgs top quark Yukawa interaction, and calculate their scattering amplitudes analytically. In section III, we perform a Monte Carlo simulation for single Higgs production at the LHeC, produce the differential and total cross section, and carry out a statistical analysis to obtain constraints for λ_3 . Finally, we conclude in section IV.

II. THE ONE LOOP CORRECTION TO SINGLE HIGGS PRODUCTION AT THE LHEC

Given the tiny cross section of di-Higgs production [46], one could instead constrain the trilinear Higgs self-coupling λ_3 at the LHeC via the λ_3 induced loop corrections to the tree level single Higgs production process $e^-p \rightarrow \nu_e h j$ shown in Fig.1. We parameterize the deviation of possible new physics from SM by a single parameter κ_λ :

$$\lambda_3^{\text{SM}} h^3 \rightarrow \lambda_3 h^3 = \kappa_\lambda \lambda_3^{\text{SM}} h^3 \quad (2)$$

where the physical Higgs field h has a zero vacuum expectation value (VEV), and $\lambda_3^{\text{SM}} \approx 0.13$ is the Higgs trilinear self-coupling in the SM.

In the following, we shall identify various contributions up to NLO that are relevant for constraining the Higgs trilinear coupling.

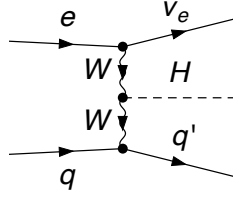


FIG. 1: The Feynman diagram of single Higgs production via W boson fusion at leading order with $q = u, c, \bar{d}, \bar{s}$ and $q' = d, s, \bar{u}, \bar{c}$ at the LHeC.

A. Trilinear Higgs self-coupling: λ_3

First, we introduce the λ_3 -dependent NLO electroweak corrections to the tree level VBF process. Their Feynman diagrams in unitary gauge are shown in Figs.2 and 3.

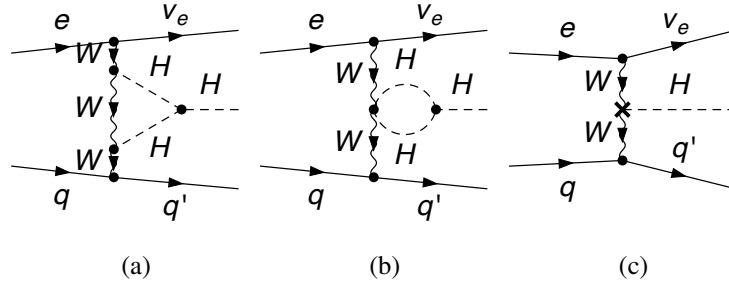


FIG. 2: The λ_3 -dependent Feynman diagrams and the corresponding counter term in unitary gauge at one-loop level with $q = u, c, \bar{d}, \bar{s}$ and $q' = d, s, \bar{u}, \bar{c}$.

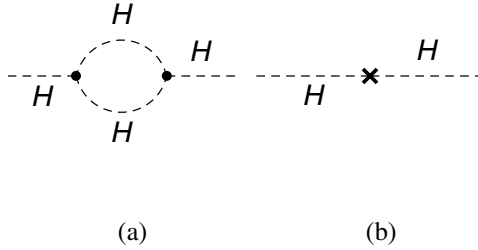


FIG. 3: λ_3 -dependent corrections to the Higgs wave function.

B. Top quark yukawa: y_t

The same final states can be produced through the top quark Yukawa coupling to the Higgs boson. Because of the large coupling strength y_t and the insertion M_t in the loop, the contribution from this channel may be sizeable and could affect the determination of the trilinear Higgs self-coupling. Therefore we shall treat it as an irreducible background and compute its contribution. As it is not straightforward to separate the contribution from top and bottom quarks in the renormalization constants, we calculate all the contribution of top and bottom quarks in the $M_b \rightarrow 0$ limit. The Feynman diagrams in the unitary gauge are shown in Fig.4. (Diagrams that vanish in the $M_b \rightarrow 0$ limit are not shown here.)

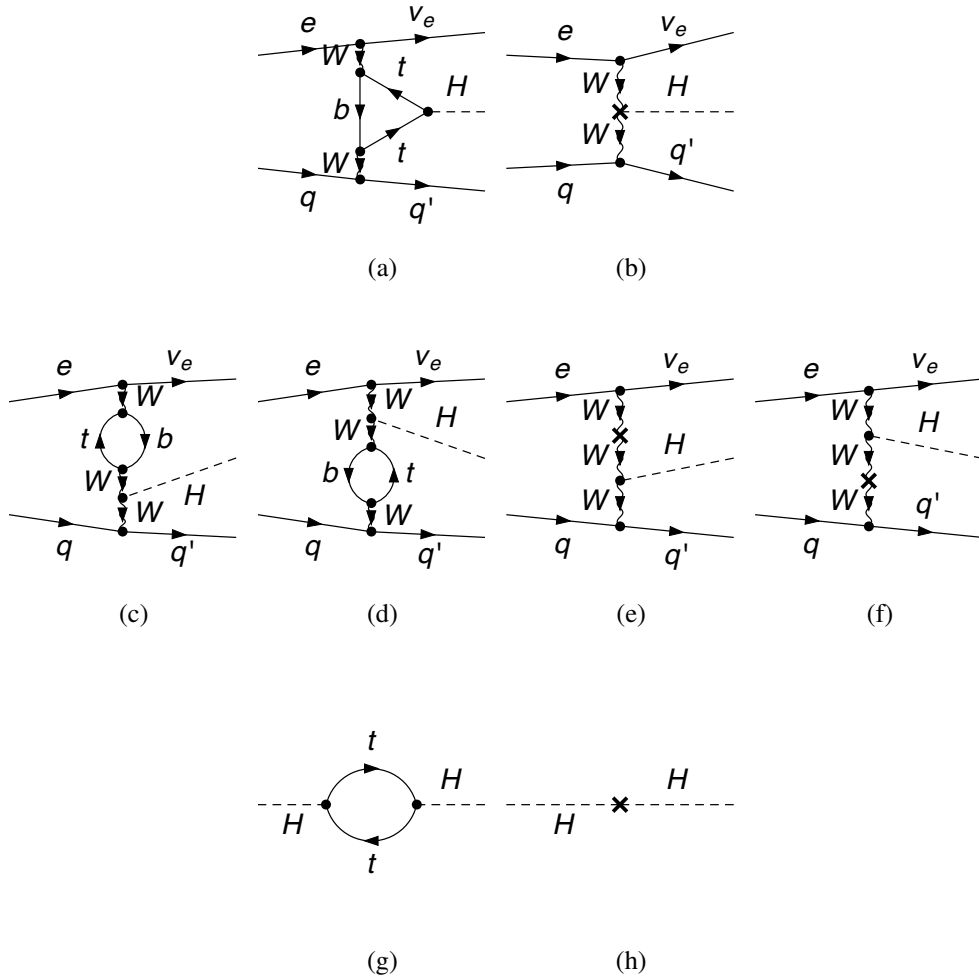


FIG. 4: Feynman diagrams with top and bottom loops and the corresponding counter terms in the unitary gauge at one loop level with $q = u, c, \bar{d}, \bar{s}$ and $q' = d, s, \bar{u}, \bar{c}$.

C. Analytical result

In this section, we give the analytical result in both on-shell and $\overline{\text{MS}}$ schemes. We shall use $\overline{\text{MS}}$ scheme in our numerical simulation in the next section. Following [48], we take e, M_H, M_W, M_Z , etc. as input parameters, and h to have a zero VEV. We do not show diagrams with Goldstone bosons in Figs.2 and 4, but for the convenience of the calculation we restore those diagrams and work in Feynman gauge.

We denote the momenta of the electron, incoming parton, Higgs boson, electron neutrino and outgoing parton by p_{1-5} respectively. The Mandelstam variables are defined as $S_{ij} \equiv (p_i + p_j)^2$, $T_{ij} \equiv (p_i - p_j)^2$. In this work the masses of u, c, d, s quarks are neglected. The CKM matrix elements $V_{ub}, V_{cb}, V_{td}, V_{ts}$ are also taken to be zero.

We expand the amplitude \mathcal{M}_q of our process in powers of $g_W \equiv \sqrt{\frac{4\pi\alpha_e}{\sin^2\theta_W}}$ as

$$\mathcal{M}_q = g_W^3 \mathcal{M}_q^{(0)} + g_W^5 \mathcal{M}_q^{(1)} + \dots, \quad (3)$$

where q stands for the incoming parton, α_e is the fine structure constant and $\theta_W \equiv \arccos \frac{M_W}{M_Z}$ is the Weinberg angle. The squared amplitude is then given by

$$\begin{aligned} & \frac{1}{4} \sum_{\text{spin}} \frac{1}{3} \sum_{\text{color}} |\mathcal{M}_q|^2 \\ &= \frac{1}{16} g_W^6 M_W^2 \frac{1}{(T_{14} - M_W^2)^2 (T_{25} - M_W^2)^2} \mathcal{F}_q^{(1)} \\ &+ \frac{3M_H^2}{256\pi^2} g_W^8 \frac{1}{(T_{14} - M_W^2)^2 (T_{25} - M_W^2)^2} \times G_\lambda \\ &- \frac{N_c M_t^2}{256\pi^2} g_W^8 \frac{1}{(T_{14} - M_W^2)^2 (T_{25} - M_W^2)^2} \times G_{t+b}^{(3)} \\ &+ \left[\frac{N_c M_W^2}{256\pi^2} g_W^8 \frac{1}{(T_{14} - M_W^2)^3 (T_{25} - M_W^2)^2} \times G_{t+b}^{(14)} + 14 \leftrightarrow 25 \right] \\ &+ \dots \end{aligned} \quad (4)$$

The spin-summed fermion chains $\mathcal{F}_q^{(1)}$ are

$$\begin{aligned} \mathcal{F}_{u,c}^{(1)} &= 4S_{12}S_{45} \\ \mathcal{F}_{\bar{d},\bar{s},\bar{b}}^{(1)} &= 4T_{15}T_{24} \\ \mathcal{F}_{u,c}^{(2)} &= (S_{12} + S_{45})(S_{12}S_{45} + T_{15}T_{24} - T_{14}T_{25}) + 2S_{12}S_{45}(T_{15} + T_{24}) \\ \mathcal{F}_{\bar{d},\bar{s},\bar{b}}^{(2)} &= (T_{15} + T_{24})(S_{12}S_{45} + T_{15}T_{24} - T_{14}T_{25}) + 2T_{15}T_{24}(S_{12} + S_{45}) \end{aligned} \quad (5)$$

where $q = u, c, \bar{d}, \bar{s}, \bar{b}$ is the incoming parton. The κ_λ dependent term G_λ reads

$$G_\lambda = \left[\left(C_{00} - \frac{1}{4} B_0 - M_W^2 C_0 \right) \mathcal{F}_q^{(1)} - C_{12} \mathcal{F}_q^{(2)} \right] \kappa_\lambda - \frac{3}{8} \kappa_\lambda^2 M_H^2 B'_0 \mathcal{F}_q^{(1)}. \quad (6)$$

Note that the contribution from κ_λ dependent counter terms vanishes. G_λ takes the same form in both OS and $\overline{\text{MS}}$ schemes, but the quantities on which it depends are generally renormalization scheme dependent. The contribution from top and bottom quarks, in the $M_b \rightarrow 0$ limit, is given by

$$\begin{aligned} G_{t+b}^{(3)} &= \left\{ 4C_{00}^{(t)} - 2B_0(T_{25}, M_b^2, M_t^2) - 2(M_t^2 - T_{14})C_0^{(t)} + \frac{1}{2} (M_H^2 + 5T_{14} - T_{25}) C_1^{(t)} \right. \\ &\quad + \frac{1}{2} (-3M_H^2 + 3T_{14} + T_{25}) C_2^{(t)} \\ &\quad - \frac{1}{2} \left[(4M_t^2 - M_H^2) B_0^{(t)} - B_0^{(t)} \right] \\ &\quad \left. + \text{CT}_{t+b}^{(3)} \right\} \mathcal{F}_q^{(1)} \\ &\quad - (C_1^{(t)} + C_2^{(t)} + 4C_{12}^{(t)}) \mathcal{F}_q^{(2)} \\ G_{t+b}^{(14)} &= \left[-4B_{00}(T_{14}, M_b^2, M_t^2) + 2(M_t^2 - T_{14})B_0(T_{14}, M_b^2, M_t^2) - 2T_{14}B_1(T_{14}, M_b^2, M_t^2) + \text{CT}_{t+b}^{(14)} \right] \mathcal{F}_q^{(1)} \end{aligned} \quad (7)$$

with contributions from counter terms [48]

$$\begin{aligned} \text{CT}_{t+b}^{(3)}|_{\text{OS}} &= 2 \frac{-16\pi^2 M_W^2}{N_c g_W^2 M_t^2} \left[\left(\delta Z_e - \frac{\delta s}{s} + \frac{1}{2} \frac{\delta M_W^2}{M_W^2} + \frac{1}{2} \delta Z_H + \delta Z_W \right) - \frac{1}{2} \delta Z_H \right]_{t+b} \\ \text{CT}_{t+b}^{(3)}|_{\overline{\text{MS}}} &= \frac{1}{2} \left(\frac{2}{4-D} \right) \\ \text{CT}_{t+b}^{(14)}|_{\text{OS}} &= \frac{32\pi^2}{N_c g_W^2} (-1) \left[\delta Z_W (T_{14} - M_W^2) - \delta M_W^2 \right]_{t+b} \\ \text{CT}_{t+b}^{(14)}|_{\overline{\text{MS}}} &= \left(\frac{2}{3} T_{14} - M_t^2 \right) \left(\frac{2}{4-D} \right) \end{aligned} \quad (8)$$

where the subscript $t + b$ represents the contribution from the top and bottom quarks, D is the dimension of space-time and $\delta Z_e, \delta Z_H, \delta Z_W, \delta s, \delta M_W^2$ are renormalization constants in the on-shell scheme. Detailed expressions of these renormalization constants can be found in [48] (Note that, at one loop level, all the renormalization constants in the above equations are independent of κ_λ except for δZ_H , whose contribution cancels out in the final result.) B_0, B'_0, C_x (e.g. $C_{00}, C_1,$

etc.) are scalar integrals

$$\begin{aligned}
C_x &= C_x(T_{14}, M_H^2, T_{25}, M_W^2, M_H^2, M_H^2) \\
B_0 &= B_0(M_H^2, M_H^2, M_H^2) \\
B'_0 &= \left. \frac{\partial}{\partial s} B_0(s, M_H^2, M_H^2) \right|_{s=M_{H,\text{ph}}^2}
\end{aligned} \tag{9}$$

and

$$\begin{aligned}
C_x^{(t)} &= C_x(T_{14}, M_H^2, T_{25}, M_b^2, M_t^2, M_t^2) \\
B_0^{(t)} &= B_0(M_H^2, M_t^2, M_t^2) \\
B_0'^{(t)} &= \left. \frac{\partial}{\partial s} B_0(s, M_t^2, M_t^2) \right|_{s=M_{H,\text{ph}}^2}.
\end{aligned} \tag{10}$$

Here $M_{H,\text{ph}}$ is the physical mass of Higgs boson while values of other mass parameters, e.g. M_H , depend on the renormalization scheme used.

The *FeynArts*, *FormCalc* and *LoopTools* suite of packages [49, 50] is used to produce the analytical result in this section and the numerical result in Sec. III. As a cross check, we repeat the calculation with *FeynCalc* [51, 52] and obtain the same result. Gauge invariance is verified by working in the general R_ξ gauge and making sure that no gauge parameter dependence remains in the final result.

III. MONTE CARLO SIMULATION

The squared amplitude in Eq.4 can be turned into the NLO cross section σ_λ for the process $e^-p \rightarrow \nu_e h j$ after integration over the phase space of the final states. We use *Vegas* algorithm implemented in Cuba library [53] to perform the numerical integration in our simulation at the parton-level. The following basic cuts are adopted:

$$\begin{aligned}
p_T^j &> 20 \text{ GeV} \\
|\eta_j| &< 5, |\eta_\ell| < 5 \\
\not{E}_T &> 5 \text{ GeV}.
\end{aligned} \tag{11}$$

With beam energies being 7 TeV and 60 GeV for the proton and electron, the cross section of the process $e^-p \rightarrow \nu_e h j$ is 80.16 fb at leading order. The contribution from the top and bottom

quarks turns out to be -1.01 fb. The *Vegas* phase space integration is cross checked with *MadGraph5_v2.6.5* [54], which gives the consistent result. In Fig.5, we show the cross section σ_λ as a function of κ_λ . The quadratic form can be traced back to the κ_λ and $(\kappa_\lambda)^2$ terms in Eq.6.

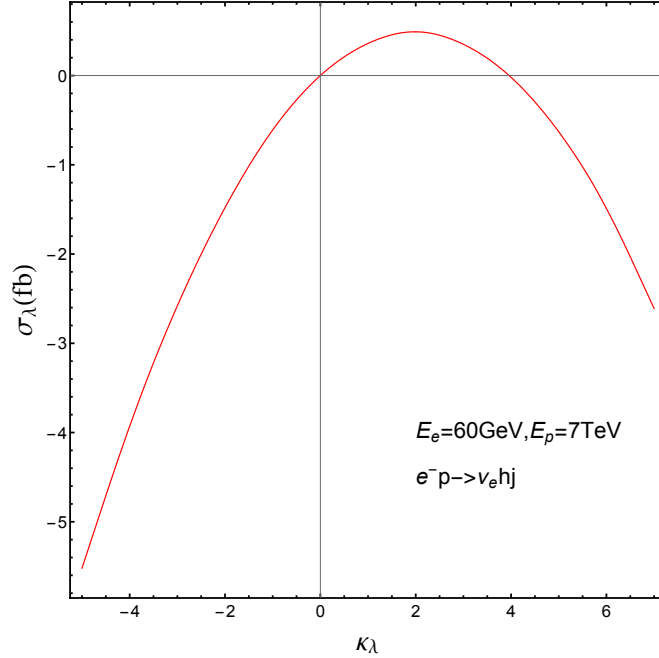


FIG. 5: The cross section σ_λ of the one-loop corrections varying with κ_λ .

One way to show the significance of κ_λ is via the differential distributions of characteristic kinematic variables, such as the azimuthal angle $\phi_{\cancel{E}_T j}$, the Higgs transverse momentum p_T^h , etc. Unfortunately, the discrimination between distributions for various processes relies heavily on the effect of threshold Sommerferld enhancement, which is absent in the case of loop corrections with the Higgs trilinear self-coupling [39]. This is very well illustrated in Fig.6 even when κ_λ is varied in a very wide range. The distributions are normalized to reflect only the difference in shape.

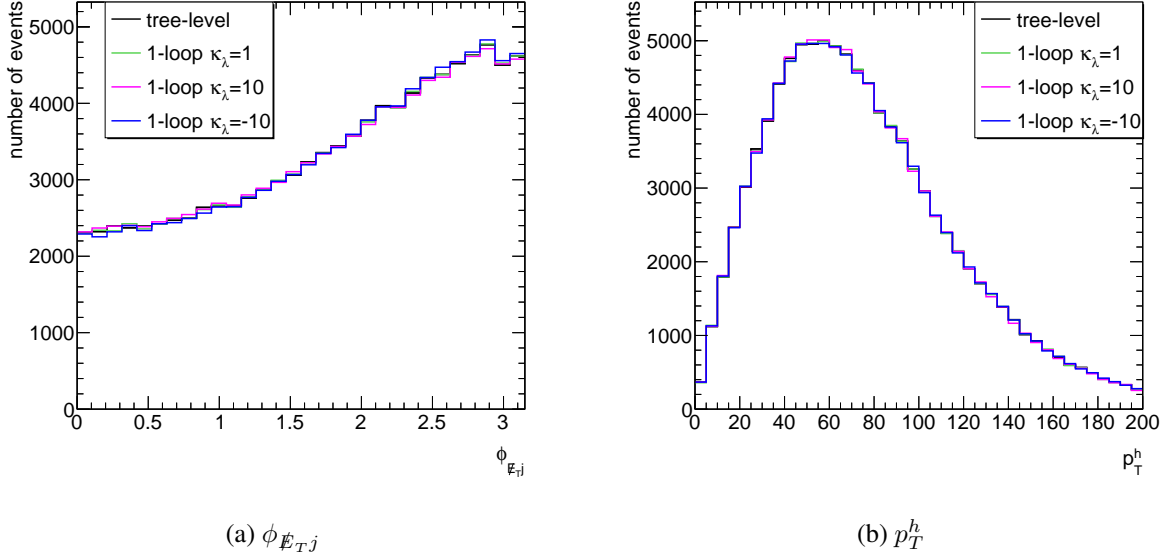


FIG. 6: The normalized $\phi_{E_T j}$ (left panel) and p_T^h (right panel) distributions with various κ_λ .

As there is little difference in shapes of distributions, we seek to identify the anomalous Higgs self interaction from SM processes using their normalizations. This can be done with the χ^2 method, in which the deviation between BSM and SM cross sections are described by

$$\chi^2 = \left(\frac{\sigma_{\kappa_\lambda \neq 1} - \sigma_{\kappa_\lambda = 1}}{\sqrt{\sigma_{\kappa_\lambda = 1}}} \right)^2 \cdot \mathcal{L}, \quad (12)$$

where $\sigma_{\kappa_\lambda = 1}$ is the production cross section of the $e^- p \rightarrow \nu_e h j$ with $\kappa_\lambda = 1$, while $\sigma_{\kappa_\lambda \neq 1}$ contains the anomalous κ_λ contribution. \mathcal{L} is the integrated luminosity. We apply the χ^2 method to the $H \rightarrow b\bar{b}$ decay channel for its large branch ratio ($BR(h \rightarrow b\bar{b}) \approx 58\%$) [55]. The results are shown in Fig.7, in which the solid blue, red and magenta curves correspond to integrated luminosities of 1, 2 and 3 ab^{-1} respectively. The limits on κ_λ at 95% C.L. are shown in the figure and listed in Table.I. We find that κ_λ is better constrained with the increase of the integrated luminosity. The most stringent limits on κ_λ is $[-0.10, 4.07]$, with $\mathcal{L} = 3 \text{ ab}^{-1}$.

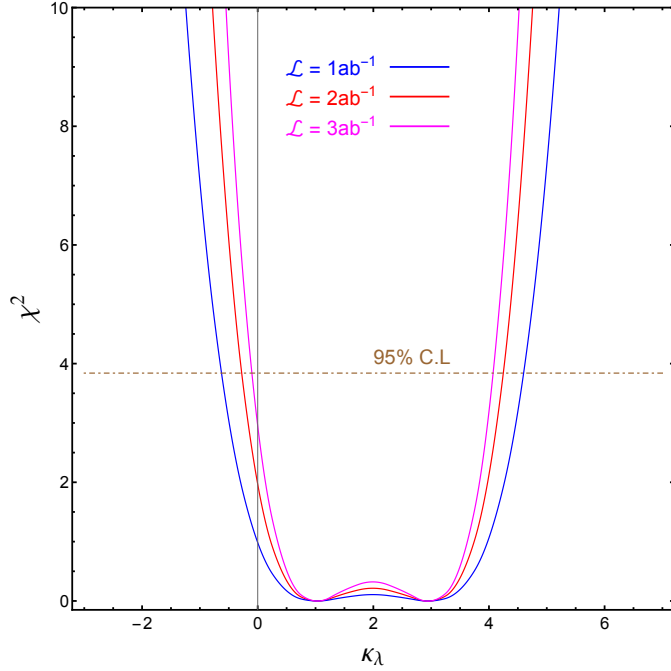


FIG. 7: The 95% C.L bounds on κ_λ for various integrated luminosities.

| The integrated Inuminosity | Bounds of the κ_λ |
|-----------------------------------|--------------------------------|
| $\mathcal{L} = 1 \text{ ab}^{-1}$ | [-0.63, 4.61] |
| $\mathcal{L} = 2 \text{ ab}^{-1}$ | [-0.28, 4.25] |
| $\mathcal{L} = 3 \text{ ab}^{-1}$ | [-0.11, 4.08] |

TABLE I: The 95% C.L bounds on κ_λ for various integrated luminosities.

The above results are obtained without considering any background other than the κ_λ independent contribution to the process $e^-p \rightarrow \nu_e h j$ up to NLO. For example, some processes with no Higgs produced are not included. Fortunately, deep inelastic scattering machines, e.g. LHeC, and FCC-eh have great potential for high precision Higgs physics. The measurement of $H \rightarrow b\bar{b}$ has reached a precision of $\mathcal{O}(1\%)$ [56, 57], which is good enough for probing the Higgs self-coupling at NLO. If we assume 10% of the decays survives the event selection cuts [45], and use the background estimate from the same reference (where the 1-loop QCD correction to VBF processes at percent level [58] is not included, which has negligible effect on our result), the bounds in Table.I are then broadened to [-2.65, 6.62], [-1.95, 5.93] and [-1.59, 5.57] with 1 ab^{-1} , 2 ab^{-1} and 3 ab^{-1} integrated luminosities respectively. These results can be improved if the background in the measurement could be further reduced.

IV. CONCLUSION

In this paper, we study the significance of the Higgs trilinear coupling through the single Higgs production process $e^-p \rightarrow \nu_e h j$ at the LHeC. The analytical calculation is carried out up to one loop level for both λ_3 dependent and independent intermediate states. The analytical results are then used in the Monte Carlo simulation to produce numerically the cross section at various κ_λ , which allows us to quantify the deviation of the cross section from the SM case ($\kappa_\lambda = 1$) in a χ^2 statistic analysis. From this analysis we find that the 95% C.L. bound for κ_λ is $[-1.95, 5.93]$ with a 2 ab^{-1} integrated luminosity, after assuming a signal surviving ratio of 10%. This is a significant improvement compared with the current experimental result. We expect the result to be improved with more accurate measurement of Higgs decays.

Acknowledgments

We thank Dr. Chen Shen, Prof. Uta Klein and LHeC Higgs & Top group for helpful discussion. The work is supported in part by the National Science Foundation of China (11875232) and the Zhejiang University Fundamental Research Funds for the Central Universities. KW is also supported by Zhejiang University K.P Chao High Technology Development Foundation.

-
- [1] ATLAS, G. Aad *et al.*, “Observation of a new particle in the search for the Standard Model Higgs boson with the ATLAS detector at the LHC,” *Phys. Lett.* **B716** (2012) 1–29, arXiv:1207.7214 [hep-ex].
- [2] CMS, S. Chatrchyan *et al.*, “Observation of a new boson at a mass of 125 GeV with the CMS experiment at the LHC,” *Phys. Lett.* **B716** (2012) 30–61, arXiv:1207.7235 [hep-ex].
- [3] ATLAS, CMS, G. Aad *et al.*, “Combined Measurement of the Higgs Boson Mass in pp Collisions at $\sqrt{s} = 7$ and 8 TeV with the ATLAS and CMS Experiments,” *Phys. Rev. Lett.* **114** (2015) 191803, arXiv:1503.07589 [hep-ex].
- [4] CMS, V. Khachatryan *et al.*, “Constraints on the spin-parity and anomalous HVV couplings of the Higgs boson in proton collisions at 7 and 8 TeV,” *Phys. Rev.* **D92** 1, (2015) 012004, arXiv:1411.3441 [hep-ex].

- [5] ATLAS, G. Aad *et al.*, “Search for a CP-odd Higgs boson decaying to Zh in pp collisions at $\sqrt{s} = 8$ TeV with the ATLAS detector,” *Phys. Lett.* **B744** (2015) 163–183, arXiv:1502.04478 [hep-ex].
- [6] ATLAS, CMS, G. Aad *et al.*, “Measurements of the Higgs boson production and decay rates and constraints on its couplings from a combined ATLAS and CMS analysis of the LHC pp collision data at $\sqrt{s} = 7$ and 8 TeV,” *JHEP* **08** (2016) 045, arXiv:1606.02266 [hep-ex].
- [7] ATLAS, T. A. collaboration, “Cross-section measurements of the Higgs boson decaying to a pair of tau leptons in proton–proton collisions at $\sqrt{s} = 13$ TeV with the ATLAS detector,”.
- [8] ATLAS, T. A. collaboration, “Observation of $H \rightarrow b\bar{b}$ decays and VH production with the ATLAS detector,”.
- [9] CMS, A. M. Sirunyan *et al.*, “Search for Higgs boson pair production in the $\gamma\gamma b\bar{b}$ final state in pp collisions at $\sqrt{s} = 13$ TeV,” arXiv:1806.00408 [hep-ex].
- [10] ATLAS, M. Aaboud *et al.*, “Search for Higgs boson pair production in the $\gamma\gamma b\bar{b}$ final state with 13 TeV pp collision data collected by the ATLAS experiment,” arXiv:1807.04873 [hep-ex].
- [11] ATLAS, M. Aaboud *et al.*, “Search for pair production of Higgs bosons in the $b\bar{b}b\bar{b}$ final state using proton-proton collisions at $\sqrt{s} = 13$ TeV with the ATLAS detector,” arXiv:1804.06174 [hep-ex].
- [12] U. Baur, T. Plehn, and D. L. Rainwater, “Measuring the Higgs boson self coupling at the LHC and finite top mass matrix elements,” *Phys. Rev. Lett.* **89** (2002) 151801, arXiv:hep-ph/0206024 [hep-ph].
- [13] U. Baur, T. Plehn, and D. L. Rainwater, “Determining the Higgs boson selfcoupling at hadron colliders,” *Phys. Rev.* **D67** (2003) 033003, arXiv:hep-ph/0211224 [hep-ph].
- [14] U. Baur, T. Plehn, and D. L. Rainwater, “Probing the Higgs selfcoupling at hadron colliders using rare decays,” *Phys. Rev.* **D69** (2004) 053004, arXiv:hep-ph/0310056 [hep-ph].
- [15] M. Moretti, S. Moretti, F. Piccinini, R. Pittau, and A. D. Polosa, “Higgs boson self-couplings at the LHC as a probe of extended Higgs sectors,” *JHEP* **02** (2005) 024, arXiv:hep-ph/0410334 [hep-ph].
- [16] M. J. Dolan, C. Englert, and M. Spannowsky, “Higgs self-coupling measurements at the LHC,” *JHEP* **10** (2012) 112, arXiv:1206.5001 [hep-ph].
- [17] J. Baglio, A. Djouadi, R. Gröber, M. M. Mühlleitner, J. Quevillon, and M. Spira, “The measurement of the Higgs self-coupling at the LHC: theoretical status,” *JHEP* **04** (2013) 151, arXiv:1212.5581

- [hep-ph].
- [18] F. Goertz, A. Papaefstathiou, L. L. Yang, and J. Zurita, “Measuring the Higgs boson self-coupling at the LHC using ratios of cross sections,” in *25th Rencontres de Blois on Particle Physics and Cosmology Blois, France, May 26-31, 2013*. arXiv:1309.3805 [hep-ph].
- [19] R. Frederix, S. Frixione, V. Hirschi, F. Maltoni, O. Mattelaer, P. Torrielli, E. Vryonidou, and M. Zaro, “Higgs pair production at the LHC with NLO and parton-shower effects,” *Phys. Lett.* **B732** (2014) 142–149, arXiv:1401.7340 [hep-ph].
- [20] Q.-H. Cao, Y. Liu, and B. Yan, “Measuring trilinear Higgs coupling in WHH and ZHH productions at the high-luminosity LHC,” *Phys. Rev.* **D95** 7, (2017) 073006, arXiv:1511.03311 [hep-ph].
- [21] S. Di Vita, C. Grojean, G. Panico, M. Riembau, and T. Vantalon, “A global view on the Higgs self-coupling,” *JHEP* **09** (2017) 069, arXiv:1704.01953 [hep-ph].
- [22] H. Baer, T. Barklow, K. Fujii, Y. Gao, A. Hoang, S. Kanemura, J. List, H. E. Logan, A. Nomerotski, M. Perelstein, *et al.*, “The International Linear Collider Technical Design Report - Volume 2: Physics,” arXiv:1306.6352 [hep-ph].
- [23] D. M. Asner *et al.*, “ILC Higgs White Paper,” in *Proceedings, 2013 Community Summer Study on the Future of U.S. Particle Physics: Snowmass on the Mississippi (CSS2013): Minneapolis, MN, USA, July 29-August 6, 2013*. arXiv:1310.0763 [hep-ph].
- [24] S. Di Vita, G. Durieux, C. Grojean, J. Gu, Z. Liu, G. Panico, M. Riembau, and T. Vantalon, “A global view on the Higgs self-coupling at lepton colliders,” *JHEP* **02** (2018) 178, arXiv:1711.03978 [hep-ph].
- [25] F. Maltoni, D. Pagani, and X. Zhao, “Constraining the Higgs self couplings at e^+e^- colliders,” arXiv:1802.07616 [hep-ph].
- [26] W. Yao, “Studies of measuring Higgs self-coupling with $HH \rightarrow b\bar{b}\gamma\gamma$ at the future hadron colliders,” in *Proceedings, 2013 Community Summer Study on the Future of U.S. Particle Physics: Snowmass on the Mississippi (CSS2013): Minneapolis, MN, USA, July 29-August 6, 2013*. arXiv:1308.6302 [hep-ph]. <http://www.slac.stanford.edu/econf/C1307292/docs/submittedArxivFiles/1308.6302.pdf>
- [27] A. J. Barr, M. J. Dolan, C. Englert, D. E. Ferreira de Lima, and M. Spannowsky, “Higgs Self-Coupling Measurements at a 100 TeV Hadron Collider,” *JHEP* **02** (2015) 016, arXiv:1412.7154 [hep-ph].
- [28] A. Azatov, R. Contino, G. Panico, and M. Son, “Effective field theory analysis of double Higgs boson

- production via gluon fusion,”*Phys. Rev.* **D92** 3, (2015) 035001, arXiv:1502.00539 [hep-ph].
- [29] H.-J. He, J. Ren, and W. Yao, “Probing new physics of cubic Higgs boson interaction via Higgs pair production at hadron colliders,”*Phys. Rev.* **D93** 1, (2016) 015003, arXiv:1506.03302 [hep-ph].
- [30] C.-Y. Chen, Q.-S. Yan, X. Zhao, Y.-M. Zhong, and Z. Zhao, “Probing triple-Higgs productions via $4b2\gamma$ decay channel at a 100 TeV hadron collider,”*Phys. Rev.* **D93** 1, (2016) 013007, arXiv:1510.04013 [hep-ph].
- [31] R. Contino *et al.*, “Physics at a 100 TeV pp collider: Higgs and EW symmetry breaking studies,”*CERN Yellow Rep.* 3, (2017) 255–440, arXiv:1606.09408 [hep-ph].
- [32] S. Banerjee, C. Englert, M. L. Mangano, M. Selvaggi, and M. Spannowsky, “ $hh + \text{jet}$ production at 100 TeV,”*Eur. Phys. J.* **C78** 4, (2018) 322, arXiv:1802.01607 [hep-ph].
- [33] J. Chang, K. Cheung, J. S. Lee, C.-T. Lu, and J. Park, “Higgs-boson-pair production $H(\rightarrow b\bar{b})H(\rightarrow \gamma\gamma)$ from gluon fusion at the HL-LHC and HL-100 TeV hadron collider,” arXiv:1804.07130 [hep-ph].
- [34] A. Blondel and P. Janot, “Future strategies for the discovery and the precise measurement of the Higgs self coupling,” arXiv:1809.10041 [hep-ph].
- [35] M. McCullough, “An Indirect Model-Dependent Probe of the Higgs Self-Coupling,”*Phys. Rev.* **D90** 1, (2014) 015001, arXiv:1312.3322 [hep-ph]. [Erratum: *Phys. Rev.* **D92**,no.3,039903(2015)].
- [36] C. Shen and S.-h. Zhu, “Anomalous Higgs-top coupling pollution of the triple Higgs coupling extraction at a future high-luminosity electron-positron collider,”*Phys. Rev.* **D92** 9, (2015) 094001, arXiv:1504.05626 [hep-ph].
- [37] G. Degrassi, P. P. Giardino, F. Maltoni, and D. Pagani, “Probing the Higgs self coupling via single Higgs production at the LHC,”*JHEP* **12** (2016) 080, arXiv:1607.04251 [hep-ph].
- [38] W. Bizon, M. Gorbahn, U. Haisch, and G. Zanderighi, “Constraints on the trilinear Higgs coupling from vector boson fusion and associated Higgs production at the LHC,”*JHEP* **07** (2017) 083, arXiv:1610.05771 [hep-ph].
- [39] F. Maltoni, D. Pagani, A. Shivaji, and X. Zhao, “Trilinear Higgs coupling determination via single-Higgs differential measurements at the LHC,”*Eur. Phys. J.* **C77** 12, (2017) 887, arXiv:1709.08649 [hep-ph].
- [40] J. Fleischer and F. Jegerlehner, “Radiative Corrections to Higgs Production by $e^+e^- \rightarrow ZH$ in the Weinberg-Salam Model,”*Nucl. Phys.* **B216** (1983) 469–492.

- [41] A. Denner, J. Kublbeck, R. Mertig, and M. Bohm, “Electroweak radiative corrections to $e + e^- \rightarrow HZ$,” *Z. Phys.* **C56** (1992) 261–272.
- [42] A. Denner, S. Dittmaier, M. Roth, and M. M. Weber, “Electroweak radiative corrections to $e + e^- \rightarrow \nu\bar{\nu}H$,” *Nucl. Phys.* **B660** (2003) 289–321, arXiv:hep-ph/0302198 [hep-ph].
- [43] G. Belanger, F. Boudjema, J. Fujimoto, T. Ishikawa, T. Kaneko, K. Kato, and Y. Shimizu, “Full one loop electroweak radiative corrections to single Higgs production in $e+e^-$,” *Phys. Lett.* **B559** (2003) 252–262, arXiv:hep-ph/0212261 [hep-ph].
- [44] LHeC Study Group, J. L. Abelleira Fernandez *et al.*, “A Large Hadron Electron Collider at CERN: Report on the Physics and Design Concepts for Machine and Detector,” *J. Phys.* **G39** (2012) 075001, arXiv:1206.2913 [physics.acc-ph].
- [45] T. Han and B. Mellado, “Higgs Boson Searches and the $H b \text{ anti-}b$ Coupling at the LHeC,” *Phys. Rev.* **D82** (2010) 016009, arXiv:0909.2460 [hep-ph].
- [46] M. Kumar, X. Ruan, R. Islam, A. S. Cornell, M. Klein, U. Klein, and B. Mellado, “Probing anomalous couplings using di-Higgs production in electron–proton collisions,” *Phys. Lett.* **B764** (2017) 247–253, arXiv:1509.04016 [hep-ph].
- [47] M. Kumar, X. Ruan, A. S. Cornell, R. Islam, and B. Mellado, “Double Higgs production at FCC-he and prospects for measurements of self-coupling,” *J. Phys. Conf. Ser.* **623** 1, (2015) 012017.
- [48] A. Denner, “Techniques for calculation of electroweak radiative corrections at the one loop level and results for W physics at LEP-200,” *Fortsch. Phys.* **41** (1993) 307–420, arXiv:0709.1075 [hep-ph].
- [49] T. Hahn, “Generating Feynman diagrams and amplitudes with FeynArts 3,” *Comput. Phys. Commun.* **140** (2001) 418–431, arXiv:hep-ph/0012260 [hep-ph].
- [50] T. Hahn and M. Perez-Victoria, “Automatized one loop calculations in four-dimensions and D -dimensions,” *Comput. Phys. Commun.* **118** (1999) 153–165, arXiv:hep-ph/9807565 [hep-ph].
- [51] R. Mertig, M. Bohm, and A. Denner, “FEYN CALC: Computer algebraic calculation of Feynman amplitudes,” *Comput. Phys. Commun.* **64** (1991) 345–359.
- [52] V. Shtabovenko, R. Mertig, and F. Orellana, “New Developments in FeynCalc 9.0,” *Comput. Phys. Commun.* **207** (2016) 432–444, arXiv:1601.01167 [hep-ph].
- [53] T. Hahn, “CUBA: A Library for multidimensional numerical integration,” *Comput. Phys. Commun.* **168** (2005) 78–95, arXiv:hep-ph/0404043 [hep-ph].

- [54] J. Alwall, R. Frederix, S. Frixione, V. Hirschi, F. Maltoni, *et al.*, “The automated computation of tree-level and next-to-leading order differential cross sections, and their matching to parton shower simulations,” *JHEP* **1407** (2014) 079, [arXiv:1405.0301](#) [hep-ph].
- [55] Particle Data Group, M. Tanabashi *et al.*, “Review of Particle Physics,” *Phys. Rev.* **D98** 3, (2018) 030001.
- [56] M. Klein, “Future Deep Inelastic Scattering with the LHeC,” in *From My Vast Repertoire ...: Guido Altarelli’s Legacy*, A. Levy, S. Forte, and G. Ridolfi, eds., pp. 303–347. [arXiv:1802.04317](#) [hep-ph].
- [57] FCC, A. Abada *et al.*, “FCC Physics Opportunities,” *Eur. Phys. J.* **C79** 6, (2019) 474.
- [58] B. Jager, “Next-to-leading order QCD corrections to Higgs production at a future lepton-proton collider,” *Phys. Rev.* **D81** (2010) 054018, [arXiv:1001.3789](#) [hep-ph].